**SUPPLEMENTARY INFORMATION**

Supplemental fig. 1: Generation of *angptl4* null mice.
(A) To generate *Angptl4* null mice, Velocigene technology was used to replace the entire coding sequence by a *LacZ* gene fused to the endogenous ATG. (B) Some lethality was observed during development but surviving *angptl4*$^{LacZ/LacZ}$ neonates were obtained at ~6%, compared to the 25% expected frequency.

Supplemental fig. 2: Vessel maturation in P6-P7 retinas.
(A, B) Three areas of the retinal vasculature distinguished by the degree of vessel maturation. (A) Control P7 retina stained with IB4 (red). White line delimitates the borders of area 1, mature vascular plexus, close to the optic nerve, from area 2, immature vascular plexus, characterised by increased capillaries caliber, increased vascular density and immature vessels. Dotted line points to the frontier of areas 2 and 3, or vascular front, composed of stalk and tip cells (A). Scale bar represents 150 μm. (B) Schematic representation of retinal vascular network where areas 1, 2 and 3 are represented in blue, red and green, respectively, and where quantification of filopodia bursts (arrows), branchpoints (yellow dots) and vessel diameters (yellow lines) are exemplified. (C-F) CAV-1 staining distinguishes area 1 from 2/3. (F) and (E) correspond to area 1 and area 2/3 regions in (D), respectively. IB4 (red). CAV-1 staining (green) is homogeneous in region 1 (F) and discontinuous in region 2/3 (E). Scale bar represents 50 μm.
(G-J) Control P7 retina labelled for ZO-1 (red in H-J) and IB4 (blue in G). Scale bars represent 100 μm (G-H) and 25 μm (I-J). (J) and (I) corresponds to area 1 and area 2/3 regions, respectively. Area 1 (J) associates with continuous endothelial junctions, area 2/3 (I) with discontinuous (arrows) and tortuous-like (arrowhead) junctions.

Supplemental fig. 3: Quantification of CAV-1 mRNA and protein in *angptl4*$^{+/LacZ}$ and *angptl4*$^{LacZ/LacZ}$ retinas at P7.
(A) Quantification by RT-qPCR of *Cav-1* mRNA expression, (B) Immuno-Blot of CAV-1 and actin (B, top), CAV-1 protein quantification normalized to actin (B, bottom), in *angptl4*$^{+/LacZ}$ and *angptl4*$^{LacZ/LacZ}$ retinas at P7.

Supplemental fig. 4: Retinal endothelial junctions are similar in area 3 and have a mild maturation defect in area 1 of *angptl4*-deficient mice.
Representative images of area 1 (A-D) and 3 (E-H) of P7 *angptl4*$^{+/LacZ}$ and *angptl4*$^{LacZ/LacZ}$ retinas stained with IB4 (blue) and ZO-1 (red). ZO-1 staining reveals a majority of continuous junctions in area 1 (C, D) and immature junctions in area 3 (G-H) of *angptl4*$^{+/LacZ}$ and *angptl4*$^{LacZ/LacZ}$ retinas. However, some sparse yet discontinuous endothelial junctions (arrows) are still present in area 1 of *angptl4*$^{LacZ/LacZ}$ retinas (D). Scale bar represents 50 μm.

Supplemental fig. 5: Retinal pericyte coverage is unaffected in area 1 of *angptl4*-deficient mice.
Representative images of area 1 (A-B) of P7 *angptl4*$^{+/LacZ}$ and *angptl4*$^{LacZ/LacZ}$ retinas stained with IB4 (green) and NG-2 (red). Scale bar represents 25 μm.

Supplemental fig. 6: *Angptl4* is expressed in retinal endothelial cells during oxygen-induced retinopathy.
LacZ staining shows expression of *angptl4* in endothelial cells at P12 (A), after hyperoxia-induced vaso-obliteration, and P17 (B), when neovascularisation is maximal during oxygen-induced retinopathy of the retina. A, artery; V, vein; VF, vascular front; o, optic nerve. Scale bar represents 500 μm.

**A** VelociGene *angptl4* Gene Knockout Technology

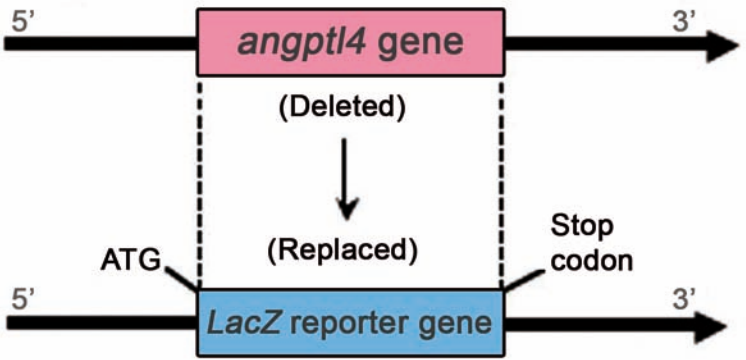


**B**

| | n | +/+ (%) | +/LacZ (%) | LacZ/LacZ (%) |
|---|---|---|---|---|
| E10.5 | 25 | 32 | 40 | 28 |
| E11.5 | 19 | 26.3 | 63.2 | 10.5 |
| E13.5 | 34 | 32.4 | 58.8 | 8.8 |
| 3 weeks | 159 | 32.1 | 61.6 | 6.3 |

Gomez *et al*, Supplemental figure 1

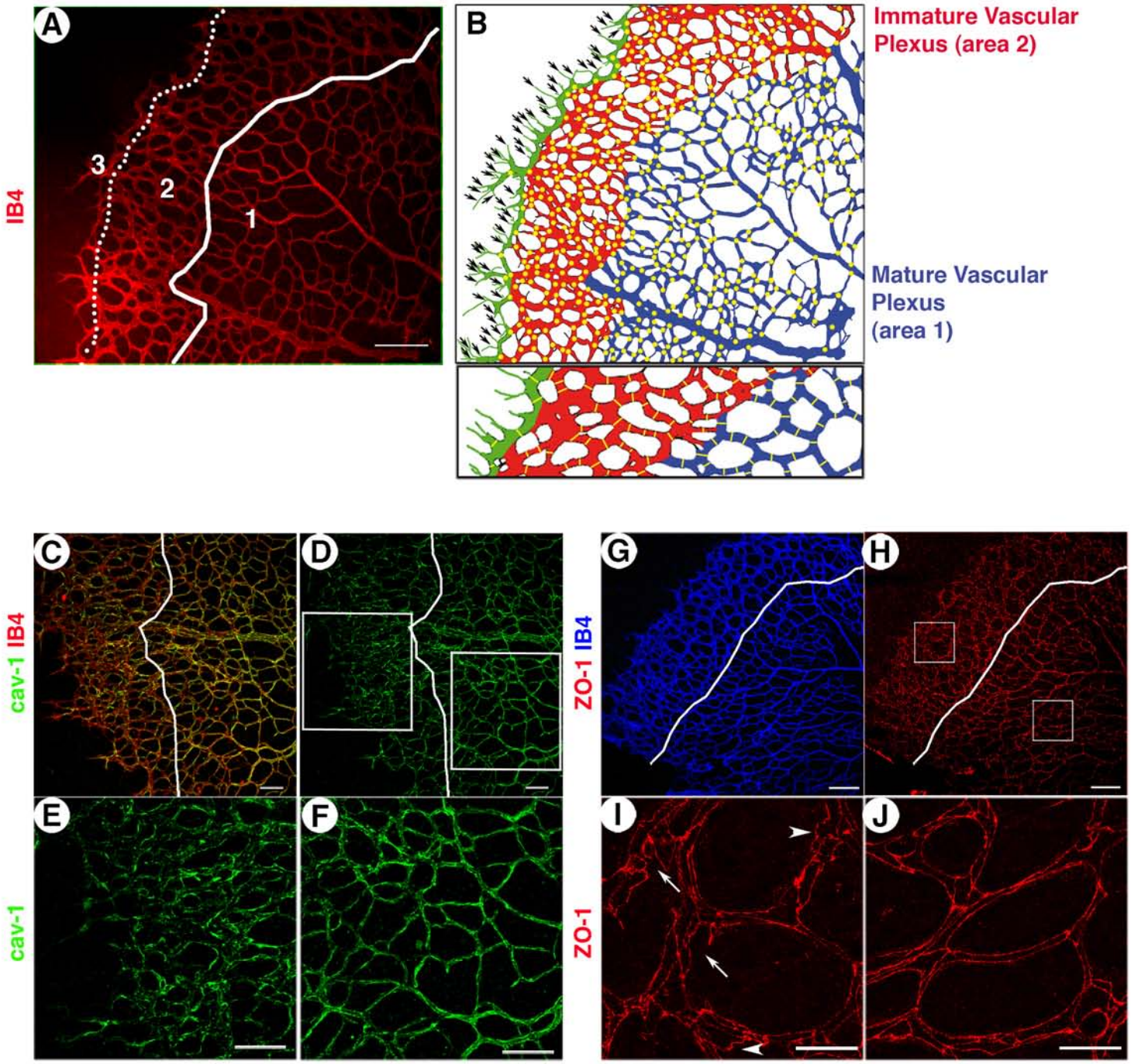


Gomez *et al*, Supplemental figure 2

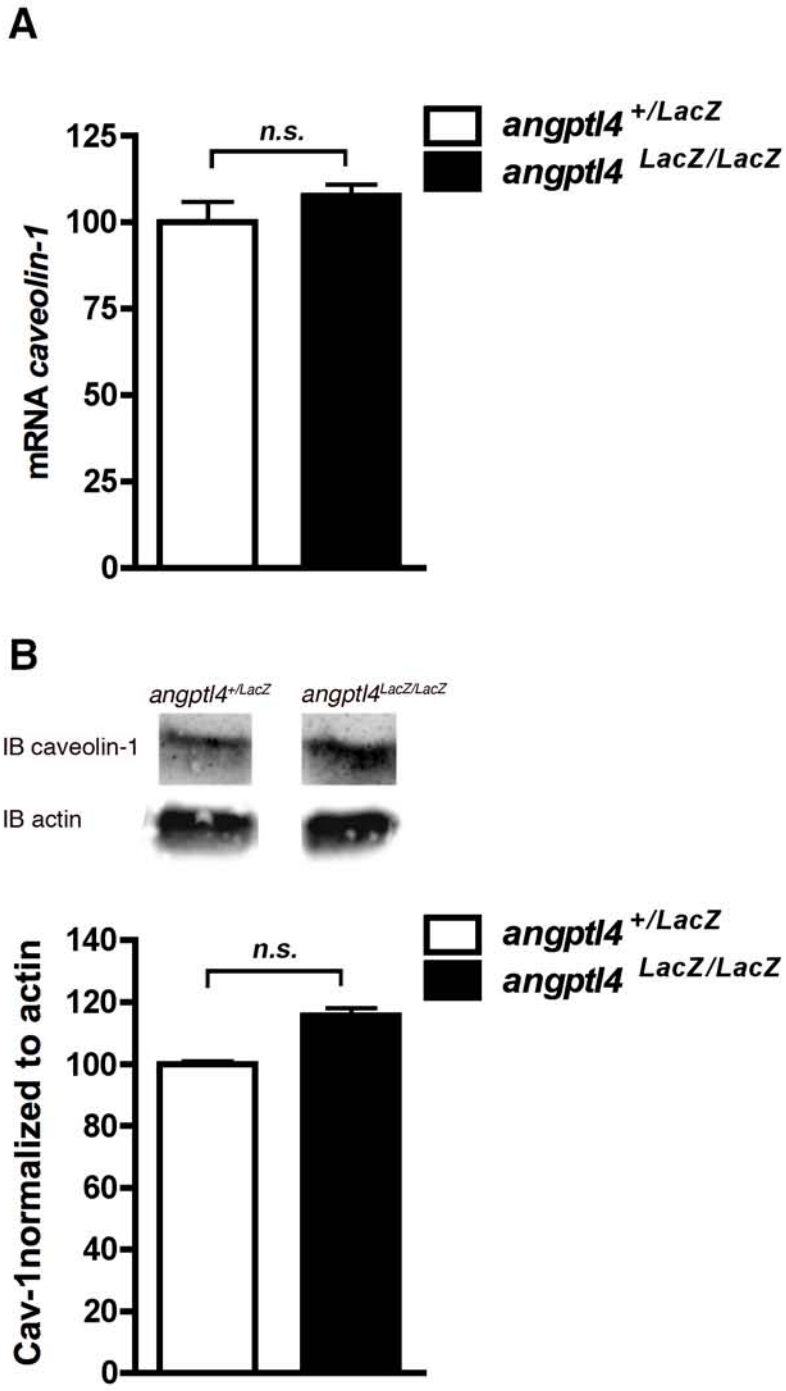


Gomez *et al*, Supplemental figure 3

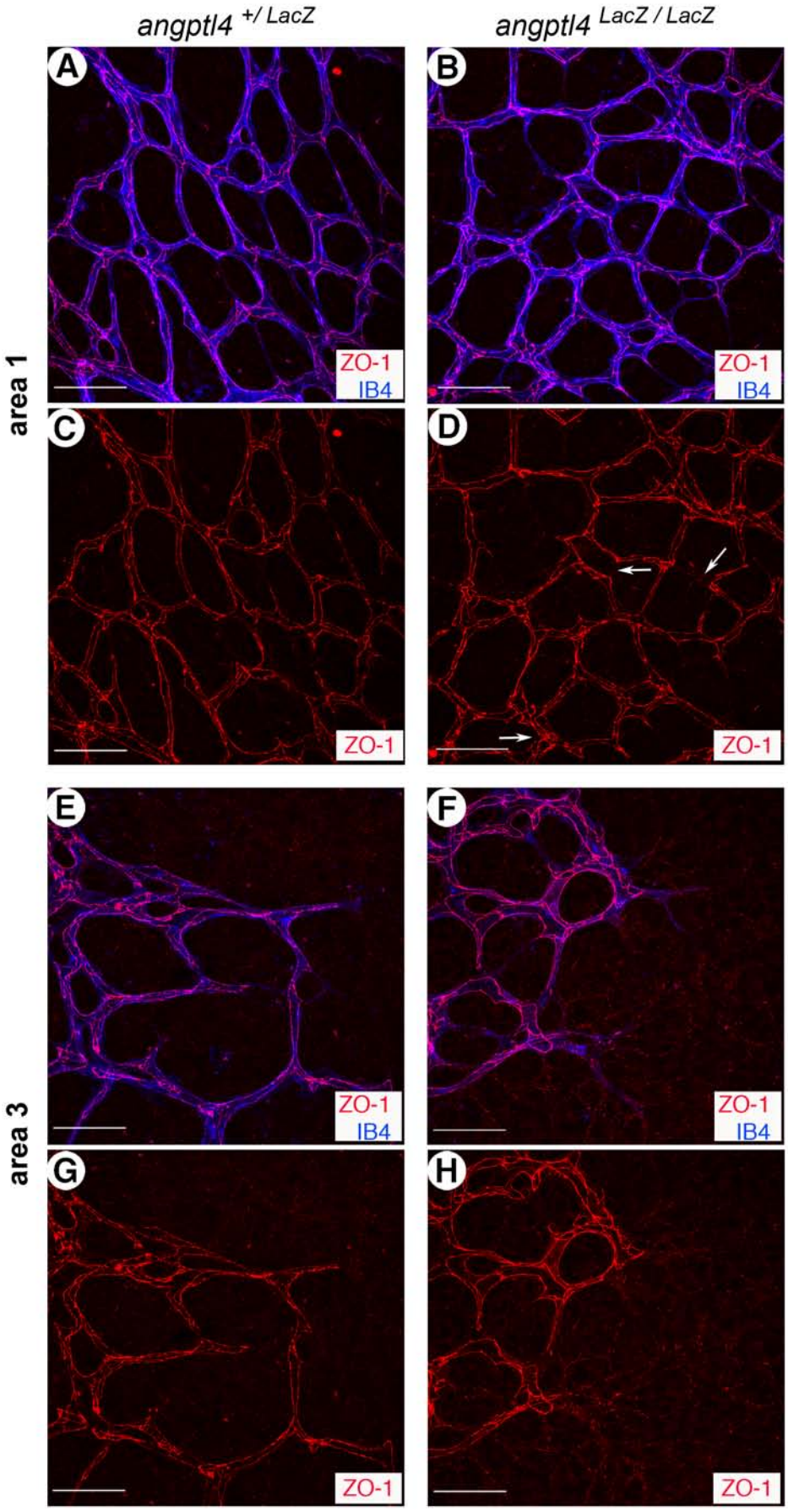


Gomez *et al*, Supplemental figure 4

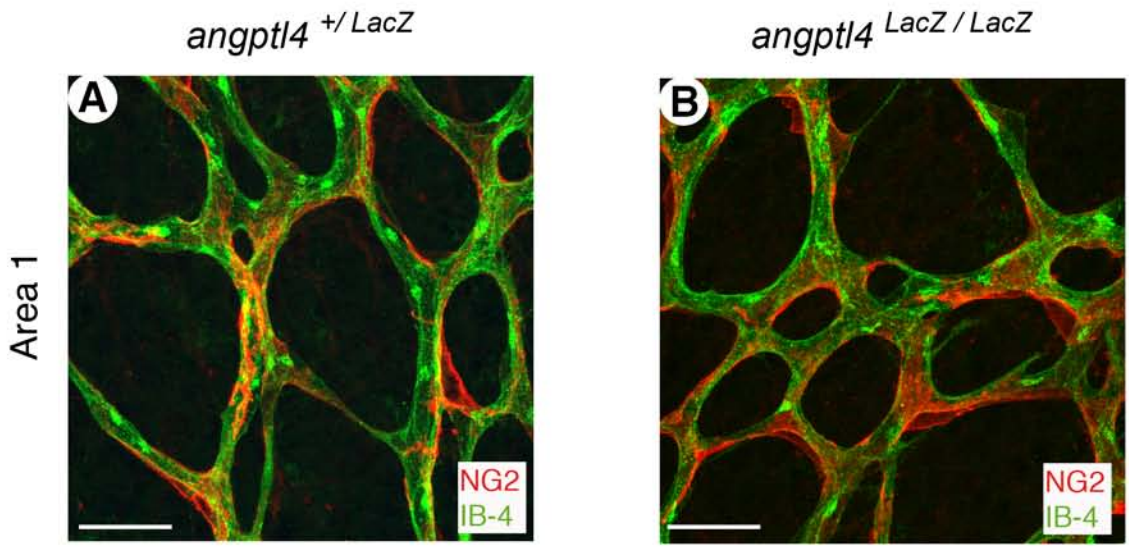


Gomez *et al*, Supplemental figure 5

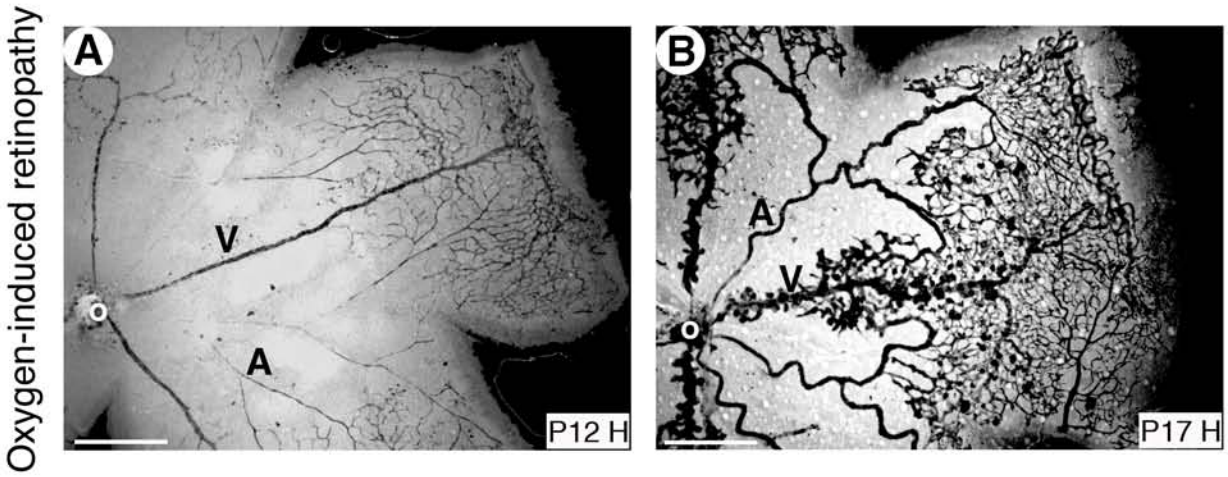


Gomez *et al*, Supplemental figure 6